———, "Effect of Boundary Conditions on the Onset of Convection,' *ibid.*, **11**, 1257 (1968).
Gallagher, A. P., and A. McD. Mercer, "On the Behaviour of Small Disturbances in Plane Couette Flow with a Temperature Gradient," *Proc. Roy. Soc. (London)*, *A286*, 117 (1965).
Gresho, P. M., and R. L. Sani, "The Stability of a Fluid Layer Subjected to a Step Change in Temperature: Transient vs. Frozen Time Analysis, *Intern J. Heat Mass Transfer*, **14**, 207 (1971).
Mahler, E. G., R. S. Schechter, and E. H. Wissler, "Stability of a Fluid with Time-Dependent Density Gradients," *Phys. Fluids*, 11, 1901 (1968).
Mayr, S. T., "Mass Transfer Enhancement in Gas-Liquid Systems due to the Marangoni Effect," Sc.D. thesis, Mass. Inst. Technol., Cambridge (1970).
Pearson, J. R. A., "On Convection Cells Induced by Surface Tension," *J. Fluid Mech.*, **4**, 489 (1958).
Ross, J. R., "The Effect of Gibbs Adsorption on Marangoni Instability," Ph.D. thesis, Mass. Inst. Technol., Cambridge (in preparation, 1972).
Scriven, L. E., and C. V. Sternling, "On Cellular Convection Driven By Surface Tension Gradients: Effects of Mean Surface Tension and Surface Viscosity," *J. Fluid Mech.*, **19**, 321 (1964).
Smith, K. A., "On Convective Instability Induced by Surface-Tension Gradients," *J. Fluid Mech.*, **24**, 401 (1966).
Spangenberg, W. G., and W. R. Rowland, "Convective Circulation in Water Induced by Evaporative Cooling," *Phys. Fluids*, **4**, 743 (1961).
Vidal, A., and A. Acrivos, "Effect of Nonlinear Temperature Profiles on the Onset of Convection Driven by Surface Tension Gradients," *Ind. Eng. Chem. Fundamentals*, **7**, 53 (1968).

Manuscript received December 9, 1971; revision received February 9, 1972; paper accepted February 9, 1972.

The Interrelationship Between Bubble Motion and Solids Mixing in a Gas Fluidized Bed

A. K. HAINES and R. P. KING

National Institute for Metallurgy Research Group, University of Natal, Durban, South Africa

E. T. WOODBURN

Department of Chemical Engineering, University of Natal, Durban, South Africa

The stochastic differential equations for particle motion in a homogeneous fluidized bed have been modified to incorporate a bubble-particle interaction. In a freely bubbling bed this interaction causes an instantaneous random step upwards when a particle collides with a bubble. In addition the particles are subject to a Brownian Motion due to particle-particle interactions and to a vertical drift velocity. The particle motion was modeled by the set of stochastic differential equations

$$dU = -U + dW$$
$$dX = (U_x + \bar{U})\,dt + S dN$$
$$dY = U_y dt$$
$$dZ = U_z dt$$

where N and W are Poisson and Wiener processes respectively. U is the velocity vector, X the vertical coordinate, Y and Z the horizontal coordinates. This set of equations has been solved and the form of the probability density function $p(x, t)$ has been obtained. Predictions are in terms of the mean bubble frequency at a point λ the average displacement associated with a particle-bubble collision, and the dense phase diffusion coefficient.

The main result is that the effective diffusion coefficient in the vertical direction is given by

$$E^* = E + \lambda/\alpha^2$$

where E is the dense phase diffusion coefficient and $1/\alpha$ is the average displacement suffered by a particle on collision with bubble.

The model was tested experimentally using random forcing function techniques. All parameters were evaluated independently; λ by direct measurement and the other two inferred from available published data. The predictions of the theory agreed well with experimental observations of the solids dispersion.

The effects of solids mixing on temperature control, heat transfer, and chemical conversion in a gas fluidized bed are well known.

Since the pioneering work of Rowe and Partridge (*1*), it has become generally accepted that the bubble phase is the chief contributor to the process of solids mixing. In spite of this acceptance, only two attempts have apparently been made to link the motion of the bubbles directly to the dispersion of the solids in the freely bubbling system (*2, 3*). The majority of investigators have followed the other general approach, using a continuous-dispersion model. Here the dispersive action of the bubbles is characterized in terms of a quasi-Fickian coefficient, generally referred to as the axial-dispersion coefficient. Values of this coefficient have been reported for various operating and design conditions (*4* to *7*), but no attempt has been made to place the model on some analytical basis. The axial dispersion model can be traced to some of the early work on Brownian motion (*8*), and its basis under conditions of large particle-displacement times and large sample populations can be regarded as the so-called Langevin stochastic differential equation. This equation describes the dynamics of a single particle. The driving force is a Gaussian white-noise process, which means that the particle can move upwards or downwards with equal probability. Houghton (*9*) has shown that a similar equation is capable of describing the movement of a particle in homogeneous fluidization. However, in a gas-fluidized or nonhomogeneous bed, the local movement of particles in the presence of bubbles is quite different. Although the Houghton model is obviously capable of handling any interparticle diffusion occurring in the dense phase, it does not account for the possibility that a particle may migrate in response to its interaction with a rising bubble.

The flow of bubbles through a fluidized bed is known to be a random process, and the following two questions arise:

1. Can a second noise process be introduced at this single-particle level that will account for this upward migration with each bubble collision and, if so,
2. Can the model be developed to a point where the final outcome can be compared with experimental observations?

The answers to both are in the affirmative.

THEORETICAL APPROACH

Stochastic Equations for Gas Fluidized Particles

The dispersion of the solids in a freely bubbling batch fluidized bed is characterized by the consideration of a particle that is to undergo small scale, continuous, random movements akin to Brownian motion and in addition to undergo discrete, upward jumps in response to rising bubbles. These jump transitions are considered to form a Poisson process, each realization constituting a staircase function, and the magnitudes of consecutive jumps S are regarded as independent and identically distributed random variables having the distribution function $F(s)$.

The formulation is based on the following points:

1. It has been suggested (*10*) on the basis of previous observations (*1, 11*) that the overall motion of the solids can be considered to consist of rapid discontinuous upward movements in regions of bubble flow, countered by a continuous slow downward drift in regions devoid of bubbles. It can be inferred that a particle in the path of an advancing bubble will interact and be displaced a discrete distance upwards or possibly even downwards. This movement has been identified with the drift of inviscid fluid elements in response to a moving object (*1*) and according to this analogy, a particle in the path of an advancing bubble experiences an increased drag force, and moves ahead of and away from the bubble. This increased drag is due to gas flowing out of the bubble cap. When the particle is alongside the bubble, it is in a region of reduced gas velocity, and it falls. As soon as the bubble has passed, the particle experiences a further drag but this time towards the bubble due to the flow of gas into the wake (*12-13*). Thus particles near the center line of the collision tend to move upwards and those away from the center line tend to move a small distance downwards. Some particles may even describe a complete loop (*14*). It is assumed that the predominant motion is in the vertical plane but the theory could easily accommodate lateral displacements as well. However, insufficient experimental data is availalbe at present to warrant such an extension. The amplitude of the vertical jump depends on the lateral position of the particle relative to the center line of motion of the bubble. The jump is a maximum for particles situated on the center line, and is negligible at distances greater than one bubble diameter from the center line (*15*).

   It has been observed that the bubble streams alter their position randomly (*16*). This means then that the horizontal distance between a known particle and a passing bubble is unknown and, therefore, the amplitude of the jump transition, a function of this distance, should similarly be regarded as a random variable.
2. Particles collide with bubbles at random points in time by virtue of their random motion through the bubbling bed. In addition local bubble frequencies also vary with time. Probe outputs reproduced by Winter (*17*) and Park et al. (*18*) tend to substantiate this proposition. Further experimental evidence is given later.
3. Rowe et al. (*19*) have shown that gas fluidized beds containing particles having a diameter less than 60 microns, initially expand to a voidage approximately 30% greater than the value of the settled bed. Thereafter, increased voidage is accounted for by the volume of bubbles within the bed as well as some further expansion of the dense phase. They found that this initial expansion permitted interparticle diffusion, and hence the solids mixing can be regarded as being due to a combination of this diffusion and the macroscopic effect of the bubbles.

This formulation is substantially the same as the qualitative picture presented in chapter 5 of the monograph by Kunii and Levenspiel (*36*). We now proceed to give a quantitative description of the model. This description is based on the theory of stochastic differential equations and the reader may consult the book by Jazwinsky (*37*) for an excellent account of this theory.

Houghton (*9*) has considered particle diffusion in homogeneous fluidization to be a Markov process. He has shown that the linearization of a force balance on a particle permits the motion of the particle to be described by the set of Langevin equations that can be written as

$$dU_i(t) = -\beta_i U_i(t)dt + dW_i(t) \quad i = 1, 2, 3 \qquad (1)$$

The driving force $W_i(t)$ is known as the Wiener process, and the process $U_i(t)$ is both Gaussian and Markov, and is called the Ornstein-Uhlenbeck process (*20*).

The particle displacement in the horizontal plane is related to the horizontal components of velocity by the differential equations

$$dX_i(t) = U_i(t)dt \quad i = 2, 3 \qquad (2)$$

Equations (1) and (2) describe the particle movement in the dense phase and the displacement in the vertical plane must allow for the collision with the bubbles. This effect is additive, and the vertical position of the particle satisfies the stochastic differential equation

$$dX_1(t) = (U_1(t) + U_m)\, dt - SdN(t) \qquad (3)$$

U_m is the rate of downward drift and is considered to be constant. Note that X_1 is considered to be positive in the downward direction.

The Poisson process $N(t)$ is a piece-wise constant function whose value increases by discrete steps at random instants of time.

It is further noted that, for a small increment of time Δt,

$$\text{prob(jump occurring)} = \lambda\Delta t + o(\Delta t) \text{ with } \lim_{\Delta t \to 0} \frac{o(\Delta t)}{\Delta t} = 0$$

The size of the jumps has a probability distribution $F(s)$. λ is the average rate at which jumps occur.

A vertical increment of $X(t)$ in a short time Δt is therefore $= (U_1 + U_m)\Delta t - s$ with probability $\lambda \Delta t p s(s)$ and equal to $(U_1 + U_m)\Delta t$ with probability $(1 - \lambda\Delta t)$.

The Kolmogorov Equation for Gas-Fluidized Particles

In the present study the statistics of the processes $W(t)$ and $N(t)$ are fundamental and therefore known. Now that the transformation equations given earlier have been formulated, the problem is to derive relationships for the joint total probability density function $p_x(\mathbf{x}, t)$ and its associated moments. These relationships can then be compared with the appropriate experimental measurements. The first step in the analysis is to set up the Kolmogorov-Feller forward equation for the process. This is an integro-partial differential equation that describes the time evolution of the joint probability density $p(\mathbf{u}, \mathbf{x}, t)$. This equation cannot be solved in general because of its complexity but various statistical properties of the motion can be obtained from it as will become apparent below. The reader is referred to (*37*), chapter 4, for a derivation and discussion of this equation for diffusion processes but for processes with finite jumps he should consult Leibowitz (*23*), Takacs (*22*), and Feller (*21*).

The processes $U_i(t)$ and $X_i(t)$, defined by the Equations (3), constitute a joint mixed Markov process. However, the Markov property is not used in this work because total density functions are being dealt with here (*24*).

If $U_i(t)$ is a three-dimensional continuous diffusional process, and $X_i(t)$ is a process having both three-dimensional continuous and one-dimensional discrete variations, this equation has the form

$$\begin{aligned}\frac{\partial p}{\partial t} = &- \sum_i \frac{\partial}{\partial u_i}(B_i(\mathbf{u})p) - \sum_i \frac{\partial}{\partial x_i}(G_i(\mathbf{x})p) \\ &+ \tfrac{1}{2} \sum_i \sum_j \frac{\partial^2}{\partial u_i\,\partial u_j}(K_{ij}(\mathbf{u})p) \\ &+ \tfrac{1}{2} \sum_i \sum_j \frac{\partial^2}{\partial x_i\,\partial x_j}(L_{ij}(\mathbf{x})p) \\ &+ \tfrac{1}{2} \sum_i \sum_j \frac{\partial^2}{\partial u_i\,\partial x_j}(M_{ij}(\mathbf{u},\mathbf{x})p) - \lambda p \\ &+ \lambda \int_0^{+\infty} p(u_1, u_2, u_3, x_1 + s, x_2, x_3, t)\,p_s(s)\,ds, \quad (5)\end{aligned}$$

where $p = (\mathbf{u}, \mathbf{x}, t)$ and $p_s(s)$ is the density function for the amplitude of the jump transition.

The derivate moments for the process $B_i(\mathbf{u}, \mathbf{x})$, $G_i(\mathbf{u}, \mathbf{x})$, $K_{ij}(\mathbf{u}, \mathbf{x})$, $L_{ij}(\mathbf{u}, \mathbf{x})$, and $M_{ij}(\mathbf{u}, \mathbf{x})$, are defined as

$$\begin{aligned}B_i(\mathbf{u}, \mathbf{x}) = \operatorname*{Lim}_{\Delta t \to 0} \frac{1}{\Delta t} \cdot E[U_i(t + \Delta t) \\ - U_i(t) \mid \mathbf{U}(t) = \mathbf{u}, \mathbf{X}(t) = \mathbf{x}]\end{aligned}$$

$$\begin{aligned}G_i(\mathbf{u}, \mathbf{x}) = \operatorname*{Lim}_{\Delta t \to 0} \frac{1}{\Delta t} \cdot E[X_i(t + \Delta t) \\ - X_i(t) \mid \mathbf{U}(t) = \mathbf{u}, \mathbf{X}(t) = \mathbf{x}]\end{aligned}$$

$$\begin{aligned}K_{ij}(\mathbf{u}, \mathbf{x}) = \operatorname*{Lim}_{\Delta t \to 0} \frac{1}{\Delta t} \cdot E[\{U_i(t + \Delta t) - U_i(t)\} \\ \cdot \{U_j(t + \Delta t) - U_j(t)\} \mid \mathbf{U}(t) = \mathbf{u}, \mathbf{X}(t) = \mathbf{x}]\end{aligned}$$

$$\begin{aligned}L_{ij}(\mathbf{u}, \mathbf{x}) = \operatorname*{Lim}_{\Delta t \to 0} \frac{1}{\Delta t} \cdot E[\{X_i(t + \Delta t) - X_i(t)\} \\ \cdot \{X_j(t + \Delta t) - X_j(t)\} \mid \mathbf{U}(t) = \mathbf{u}, \mathbf{X}(t) = \mathbf{x}]\end{aligned}$$

$$\begin{aligned}M_{ij}(\mathbf{u}, \mathbf{x}) = \operatorname*{Lim}_{\Delta t \to 0} \frac{1}{\Delta t} \cdot E[\{U_i(t + \Delta t) - U_i(t)\} \\ \cdot \{X_j(t + \Delta t) - X_j(t)\} \mid \mathbf{U}(t) = \mathbf{u}, \mathbf{X}(t) = \mathbf{x}]\end{aligned}$$

These moments are evaluated by integration of the stochastic differential equations (1), (2), and (3) over a short time interval Δt under conditions of no-jump transition.

Because the small scale velocity fluctuations in each spatial direction are statistically independent (9) it can be shown that

$$\begin{array}{llll} B_i(\mathbf{u}) = \beta_i u_i & & i = 1, 2, 3 \\ G_1(\mathbf{u}) = u_1 + U_m & & \\ G_j(\mathbf{u}) = u_j & & j = 2, 3 \\ K_{ij} \;\; = 2D_i & i = j & i, j = 1, 2, 3 \\ \quad\;\;\; = 0 & i \neq j & \\ L_{ij} \;\; = 0 & & i, j = 1, 2, 3 \\ M_{ij} \;\; = 0 & & i, j = 1, 2, 3 \end{array}$$

When these moments are substituted into Equation (5)

$$\begin{aligned}\frac{\partial p}{\partial t} + U_m \frac{\partial p}{\partial x_1} = &\sum_i \beta_i \frac{\partial u_i p}{\partial u_i} - \sum_i u_i \frac{\partial p}{\partial x_i} \\ &+ \sum_i D_i \frac{\partial^2 p}{\partial u_1^2} - \lambda p + \lambda \int_0^{+\infty} \\ &p(u_1, u_2, u_3, x_1 + s, x_2, x_3, t)p_s(s)ds \quad i = 1, 2, 3 \quad (6)\end{aligned}$$

The Distribution of the Displacement of a Gas Fluidized Particle

The Kolmogorov forward Equation (6) is partially solved by use of its Fourier transform and the method of characteristics. The following substitutions

$$\begin{array}{lll} y_1 & = x_1 - U_m t & \\ y_j & = x_j & j = 2, 3 \\ z_{1_i} & = u_i & i = 1, 2, 3 \\ z_{2_i} & = u_i + \beta_i y_i & i = 1, 2, 3 \end{array}$$

are inserted into Equation (6):

$$\begin{aligned}\frac{\partial p}{\partial t} = &\sum_i \beta_i \frac{\partial z_{1_i} p}{\partial z_{1_i}} + \sum_i D_i \left[\frac{\partial}{\partial z_{1_i}} + \frac{\partial}{\partial z_{2_i}}\right]^2 p - \lambda p \\ &+ \lambda \int_0^{+\infty} p(z_{11}, z_{12}, z_{13}, z_{21} \\ &+ \beta_1 s, z_{22}, z_{23}, t)p_s(s)ds \quad i = 1, 2, 3 \quad (7)\end{aligned}$$

The introduction instead of p of its multiple Fourier transform, defined as

$$f(\xi_{11}, \xi_{12}, \xi_{13}, \xi_{21}, \xi_{22}, \xi_{23}, t)$$

$$= \int_{-\infty}^{+\infty} \cdots \int_{-\infty}^{+\infty} p(z_{11}, \ldots, z_{13}, z_{21}, \ldots, z_{23}, t)$$

$$\exp\left(-\sum_i j(\xi_{1_i} z_{1_i} + \xi_{2_i} z_{2_i})\right)$$

$$dz_{11} \ldots dz_{13}\, dz_{21} \ldots dz_{23} \quad (8)$$

results in f satisfying the linear first-order partial differential equation

$$\frac{\partial f}{\partial t} = \sum_i \left[-\beta_i \xi_{1_i} \frac{\partial f}{\partial \xi_{1_i}}\right] - \sum_i [D_i(\xi_{1_i} + \xi_{2_i})^2 f]$$

$$-\lambda f + \lambda f \int_0^{+\infty} \exp(+j\beta_1 s \xi_{21}) ps(s)\, ds \quad (9)$$

The magnitude of a jump S is a function of the distance R between the particle and the center line of the bubble. This can be written as

$$A = g(r) \quad (10)$$

The density function $p_s(s)$ can be evaluated by use of the theorem (*25*)

$$p_s(s) = p_r(r)/|dg(r)/dr| \quad (11)$$

where $p_r(r)$ is the probability density for R.

The form of the function $g(r)$ is potentially derivable from a fluid mechanical treatment. No rigorous analysis exists, and the only known attempted description is the potential flow analogy proposed by Rowe and Partridge (*1*). However, the analogy has been shown (*1, 26*) to underpredict the particle movement and, because of this underprediction, an approximation is made on the basis of the experimental results of Woollard and Potter (*26*). This is that S is exponentially distributed and

$$p_s(s) = \alpha \exp(-\alpha s) \quad (12)$$

$$\frac{\partial f}{\partial t} = \sum_i \left[-\beta_i \xi_{1_i} \frac{\partial f}{\partial \xi_{1_i}}\right] - \sum_i [D_i(\xi_{1_i} + \xi_{2_i})^2 f]$$

$$+ \frac{\lambda f}{1 - j\xi_{21}\beta_1/\alpha} - \lambda f \quad (13)$$

This equation can now be solved for f by the method of characteristics.

At this stage, the boundary conditions have to be introduced. For local dispersion the particle can be considered to be completely free, and the boundary conditions are simply

$$t > 0 : p \to 0 \text{ as } x_1, x_2, x_3 \to \pm\infty \quad (14)$$

Equation (13) is therefore solved subject to these and the initial conditions

$$t = 0 : p(z_{11}, \ldots, z_{13}, z_{21}, \ldots, z_{23}, 0)$$

$$= \prod_i \delta(z_{1_i} - z^0{}_{1_i})\delta(z_{2_i} - z^0{}_{2_i}) \quad (15)$$

The characteristic equations are

$$\frac{dt}{1} = \frac{d\xi_{11}}{\beta_1 \xi_{11}} = \frac{d\xi_{12}}{\beta_2 \xi_{12}} = \frac{d\xi_{13}}{\beta_3 \xi_{13}}$$

$$= \frac{df}{\sum_i [-D_i(\xi_{1_i} + \xi_{2_i})^2 f] - \lambda f + \lambda f/(1 - j\xi_{21}\beta_1/\alpha)} \quad (16)$$

By integration and introduction of the initial conditions the transformed solution is

$$f = \exp\left[\sum_i \left(-j(\xi_{1_i} \exp(-\beta_i t) z^0{}_{1_i} + \xi_{2_i} z^0{}_{2_i})\right.\right.$$

$$+ D_i \left(\frac{-\xi^2{}_{1_i}}{2\beta_i} + \frac{\xi^2{}_{1_i}}{2\beta_i} \exp(-2\beta_i t) - \frac{2\xi_{1_i}\xi_{2_i}}{\beta_i}\right.$$

$$\left.\left. + \frac{2\xi_{1_i}\xi_{2_i}}{\beta_i} \exp(-\beta_i t) - \xi^2{}_{2_i} t\right)\right)$$

$$\left. - \lambda t + \lambda t/(1 - j\xi_{21}\beta_1/\alpha) \right] \quad (17)$$

Equation (17) is as far as the solution can be taken. Nevertheless, the exact form of $p_x(\mathbf{x}, t)$ is not a necessary requirement since it can be shown that for large values of t the density is asymptotically normal (*27*). Thus, all that is required here is a knowledge of the first and second moments. These can be evaluated direct by differentiation of the transformed solution (*17*).

The moments required here are defined by

$$M_k = \int_{-\infty}^{\infty} \cdots \int_{-\infty}^{\infty} x_1{}^k p(\mathbf{u}, \mathbf{x})\, d\mathbf{x}\, d\mathbf{u}$$

and are

$$M_0 = 1 \quad (18)$$

$$M_1 = (U_m - \lambda/\alpha)t \quad (19)$$

$$M_2 = 2(E_1 + \lambda/\alpha^2)t \quad (20)$$

where E_1 is given by $D_1/\beta_1{}^2$ for $t \geqq 1/\beta$.

For batch fluidization, the first moment must be zero, that is, $U_m = \lambda/\alpha$. For a bed fed continuously with solids, $U_m - \lambda/\alpha$ is equal to the average velocity of the solids through the bed.

The second moment or variance gives the dispersion of the solids in the axial direction. This dispersion results from the combined action of dense phase diffusion and bubble flow.

The density function for particle displacement can finally be written as (source at $x = 0$)

$$p_x(\mathbf{x}, t) = \frac{1}{(4\pi t)^{3/2}(E_1{}^* E_2 E_3)^{1/2}} \exp$$

$$-\left[\frac{x_1{}^2}{4E_1{}^* t} + \frac{x_2{}^2}{4E_2 t} + \frac{x_3{}^2}{4E_3 t}\right] \quad (21)$$

where

$$E_1{}^* = E_1 + \lambda/\alpha^2 \quad (22)$$

Interpretation of the Parameters Describing the Bubble Effect

The parameters λ and α are not directly measurable but are related to two that are, namely, bubble frequency and diameter.

The basic assumption in the formulation of the model is that the particle-bubble collision process is Poisson-distributed in time. It is possible then to infer that the point bubble frequency is similarly distributed and has the same mean. This inference is justified if the bubbles are assumed to be uniformly distributed in space over the region through which particles are considered to disperse.

The parameter α is clearly the inverse of the expected value of S designated $\overline{S}$. Rowe and Partridge (*1*), on the basis of photographic studies, have suggested as a crude approximation that with each bubble interaction particles can be regarded as being displaced through an average distance of one bubble diameter. It is therefore inferred that

$$\alpha = 1/D_b \quad (23)$$

The validity of this relationship can be objectively judged from an analysis of the work of Woollard and Potter (26) and from the assumption of a uniform spatial distribution of bubbles.

An examination of their data and experimental technique reveals that their graphs of particle displacement can be approximated reasonably well by the complement of the distribution function $F(s)$, that is,

$$1 - F(s) = \exp(-\alpha s) \tag{24}$$

The parameter α can therefore be estimated by use of nonlinear regression techniques (28). The best estimates by these techniques are plotted in Figure 1, which also shows the relationship given by Equation (23). As can be observed, Equation (23) is quite acceptable for an order of magnitude estimate.

EXPERIMENTAL METHOD

Design

It was proposed that the model should be tested by a comparison of the solids dispersion predicted from prior information on bubble flow and the experimental estimates obtained from the use of radioactive tracers.

The experimental method used was the correlation technique. This method consists in the excitation of the system with a random test signal and the formation of the cross-correlation function between two observed signals or an observed signal and the exciting signal. This cross-correlation function is then available for comparison with theoretically derived information.

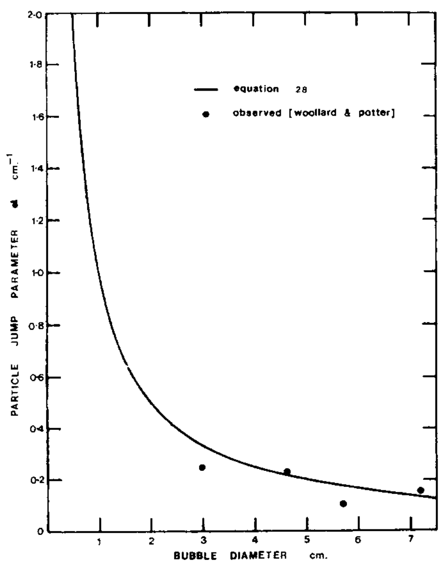

Fig. 1. Dependence of α on bubble diameter.

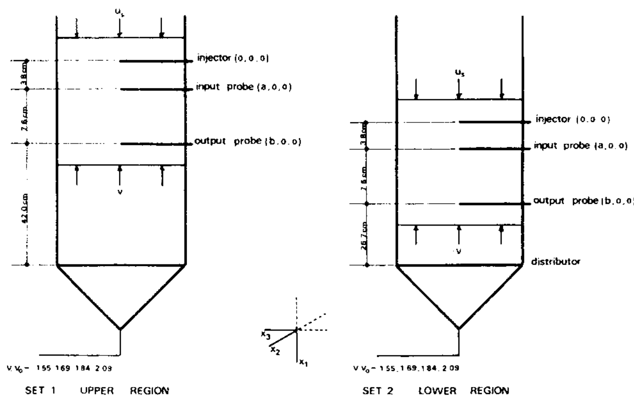

Fig. 2. Experimental conditions.

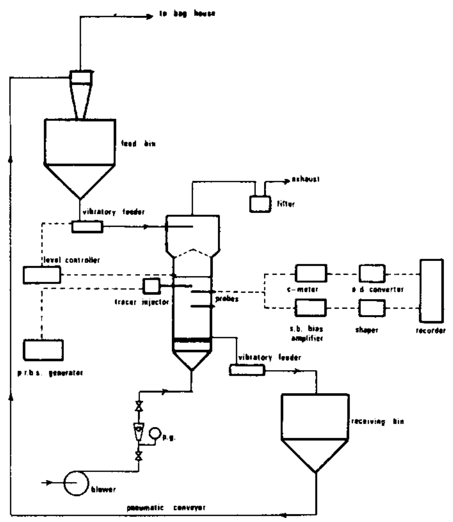

Fig. 3. Schematic diagram of apparatus.

To test the model's ability to predict solids dispersion following changes relating to bubble frequency and diameter, two sets of experiments were designed. These included the variables gas flowrate and axial position above the distributor. The conditions are shown in Figure 2.

A continuous solids-flow system was used to alleviate tracer accumulation problems.

For the situation depicted, it can be shown by well-known means that, for a time-stationary input into a linear system, the cross-correlation function between two observed signals is given by

$$R_{ab}(\tau) = g \cdot L \int_0^\infty \frac{R_{aa}(\tau - \theta)}{(4\pi E_1^* \theta^3)^{1/2}} \exp\left[-\frac{(L - U_s\theta)^2}{4E_1^*\theta}\right] d\theta. \tag{25}$$

This equation permits the prediction of the cross-correlation if the input autocorrelation and the parameters E_1^* and U_s are known. The time-stationary random source was simulated by a Pseudo Random Binary Sequence (P.R.B.S.). The advantages of these sequences have been discussed (29). In the design of a suitable P.R.B.S., the following variables were considered.

1. Signal amplitude—The amplitude of the signal was limited by consideration of cost and health. It was estimated at 0.01 millicurie of ^{140}La per gram of tracer.
2. Decision interval—This was estimated experimentally. Values used over the range of air flowrates considered are given in Table 1.
3. Period length—The sequence used in all tests was of a 7 decision period length.
4. Experiment length—This was set at the value of the maximum recording time available, that is, 1½ hours.
5. Sample interval—This was set at the minimum available, that is, 1.2 seconds.

Apparatus

A diagrammatic representation of the experimental equipment is given in Figure 3.

The column, having a nominal diameter of 9 in. and a length of 44 in., was fabricated from 3/16-in. Perspex, and was fitted with a disengagement section, 12 in. in diameter and 22 in. long. Fluidizing air entered through a conical section (60° included angle) bolted to the column.

The air distributor was sandwiched between the column and the conical inlet section. It consisted of a double layer of 3/16-in. thick Vyon, a porous plastic material having a mean pore size of 50 microns. Ambient air for fluidization was delivered by an oil-free, sliding-vane rotary blower and metered through a calibrated rotameter.

The fluidized solid material was crushed dolomite having a

TABLE 1. DECISION INTERVALS USED IN THIS WORK

Air velocity	Decision interval
v/v_0	s
1.55	20
1.69	22
1.84	24
2.09	24

TABLE 2. DISTRIBUTION OF SOLIDS

Particle size	Weight
μm	%
+210	2.59
−210 +177	3.91
−177 +149	5.59
−149 +125	8.67
−125 +106	14.05
−106 + 88	9.77
− 88 + 63	27.24
− 63 + 37	20.59
−37	7.59

particle density of 2.86 g./cm^3. The size range is shown in Table 2.

The solids were fed and removed from the column by vibratory feeders. The flowrate was fixed at 207 Kg/hr. A simple 'on-off' controller was used for the control of the bed level.

The radioactive isotope used was ^{140}La having a half-life of 40.2 hours. The principal mode of decay is by β-emission of energy 1.34 mev. The tracer was prepared by the adsorption from a solution of the isotope on a portion of the bulk solids.

An injector was designed to inject the tracer direct into the bed to simulate a point source. It consisted of a small screw conveyor operated by a fractional-horsepower motor through a reduction gearbox and plate clutch. The clutch was controlled electrically by a shift-register circuit that generated the P.R.B.S.

The tracer concentration was measured with a surface-barrier detector built into a probe that could be positioned within the bed. The detectors were operated under an 8.5 volt bias, and their output was amplified, shaped, and recorded on magnetic tape. The data were then recovered in digital form on computer cards.

RESULTS AND DISCUSSION

Dependence of λ and D_b on Gas Velocity and Bed Position

Before a comparison of theoretical and experimental estimates of solids dispersion can be made, the dependence of both λ and D_b on gas velocity and bed position must be known. The dependence of λ was evaluated experimentally since no explicit correlation is apparently available.

The bubble frequency was measured by use of a capacitance probe built into the surface-barrier detector. Its dependence on gas velocity and vertical position is shown in Figure 4. The reported values of λ are arithmetical averages taken over a period of 1 hr. These are apparently the only estimates of bubble frequency over this range of gas velocities. Nevertheless, comparison with the work of Kunii et al. (3) could be made by extrapolation. This led to predictions consistent with their observations.

The above experiments were also used to test the validity of the assumption that the basic distribution was a Poisson distribution. The probe outputs were sampled at 5-sec. intervals, and the frequency distribution of the number of bubbles registered in the interval was computed. A typical normalized distribution is shown in Figure 5. The smooth curve drawn through the distribution is the locus of the best-fit Poisson probability. The Poisson representation of the bubble frequency cannot be said to be absolutely satisfactory, but the discrepancy is not too pronounced. The Poisson representation does provide a useful description of the bubble process since its properties are well known.

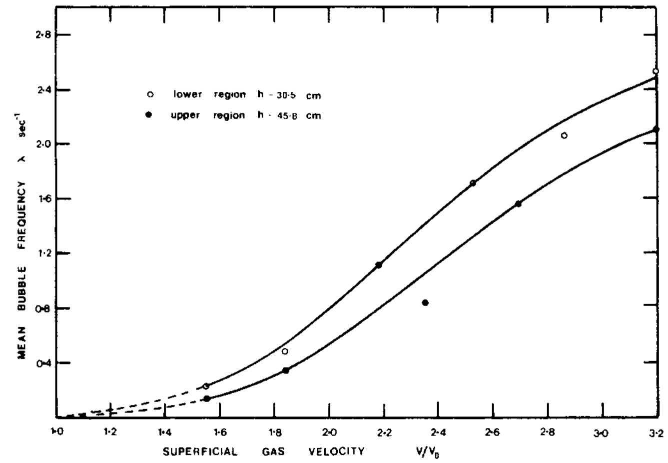

Fig. 4. Dependence of λ on gas velocity and height h.

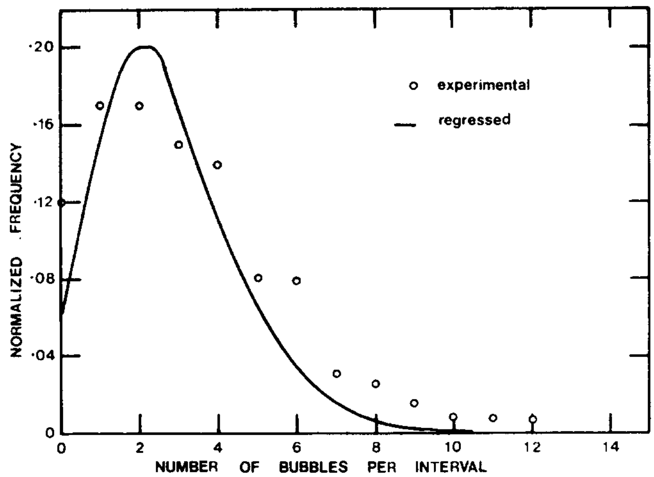

Fig. 5. Distribution of bubble counts, upper region $V/V_0 = 2.09$.

Studies of bubble growth in a gas fluidized bed are numerous. The most noteworthy data, all using porous plate distributions, have been collected by Kato and Wen (30) and plotted in terms of $D_b/\rho_p D_p(v/v_0)$ and height h. Although the data were somewhat scattered, Kato and Wen found that the bubble diameter along the axis and the height could be approximately related by the correlation of Kobayashi et al. (31).

$$D_b = 1.4\ \rho_p\ D_p\ (v/v_0)\ h \tag{26}$$

This correlation is clearly an oversimplification of the real situation but in the absence of more accurate techniques of measurement than those at present in use there is no real justification for the use of a more sophisticated correlation.

Solids Dispersion Due to Bubbles

The value of the effective axial dispersion coefficient E_1^* can now be calculated from the stochastic model by use of the independent point estimates of bubble diameter and frequency. The dependence of E_1^* on gas velocity and bed position is shown in Figure 6. The incipient

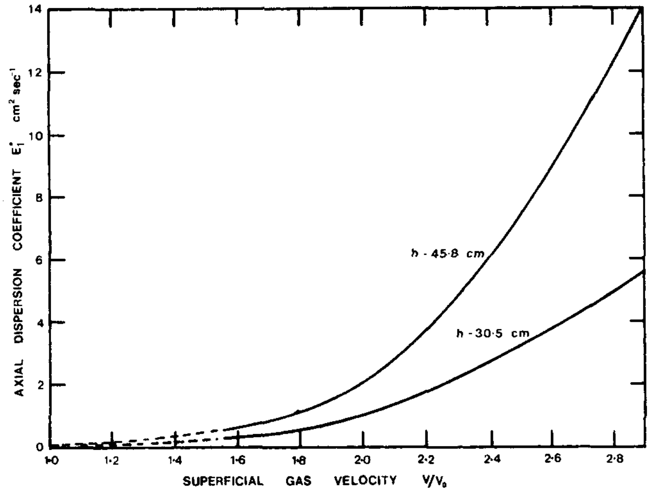

Fig. 6. Dependence of $E_1{}^*$ on gas velocity and height h.

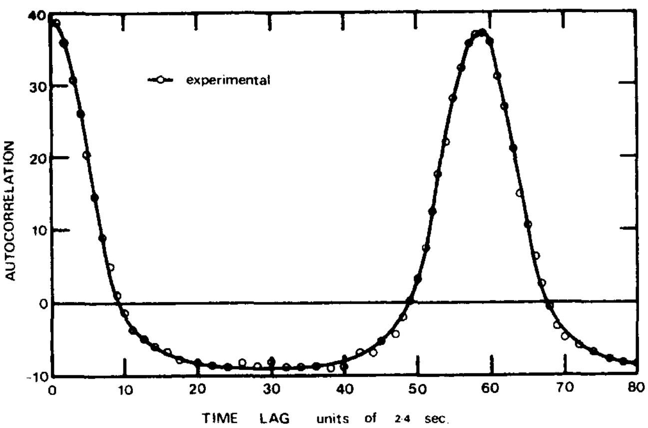

Fig. 7a. Autocorrelation function, upper region $V/V_0 = 1.55$.

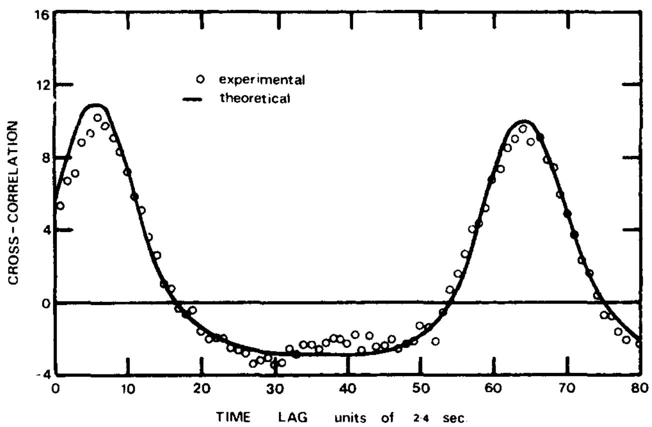

Fig. 7b. Cross-correlation function, upper region $V/V_0 = 1.55$.

fluidization velocity was measured and found to be 0.455 cm./s. The dense phase diffusion coefficient E_1 was inferred from data available in the literature (*32, 33*). An average value of 0.12 sq. cm/s was used. Over the range plotted, the shape of the curve is consistent with the observations of Gabor (*2*) and Kunii et al. (*3*). The model also predicts the hitherto unaccounted for dependence of $E_1{}^*$ on axial position, which has been observed by Littman (*5*) and Jinescu et al. (*34*).

For the quantitative comparison of the predicted dispersion with the experimental, values of $E_1{}^*$ and estimates of U_s were substituted into Equation (25) and the cross-correlation function $R_{ab}(\tau)$ was evaluated in terms of the autocorrelation $R_{aa}(\tau)$ for the various experimental conditions. These curves could then be compared with the experimental realizations. Typical curves are shown in Figures 7 to 10.

The autocorrelation functions are shown in their uncorrupted form, the noise having been removed by extrapolation (*29*). The functions are symmetrical and, although filtered, still exhibit the characteristic shape of the autocorrelation of a P.R.B.S. The cross-correlation functions are asymmetrical and displaced. The displacement can be defined as the period of time between the first crossings of the rising portions of the autocorrelation and cross-correlation function with their respective abscissae. This time was used in the estimation of the mean solids velocity U_s.

The agreement between the predicted and experimental cross-correlation functions for the upper region was found to be good over all the gas velocities considered.

For the lower region, however, the functions for the lower two gas velocities showed a discrepancy in amplitude, although the spread was consistent. The difference

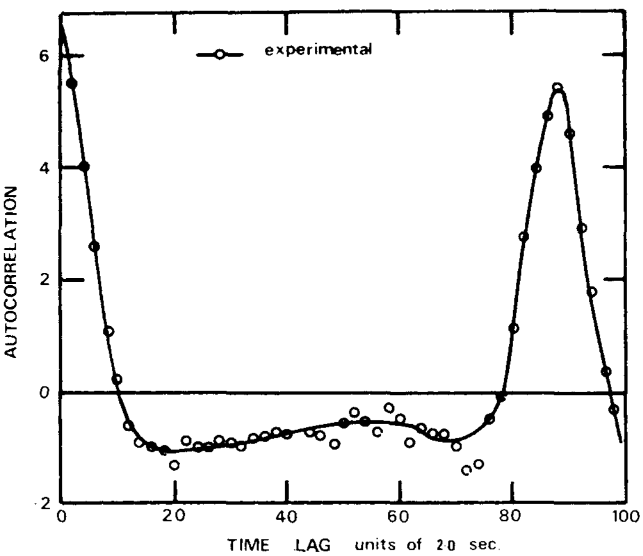

Fig. 8a. Autocorrelation function, upper region $V/V_0 = 2.09$.

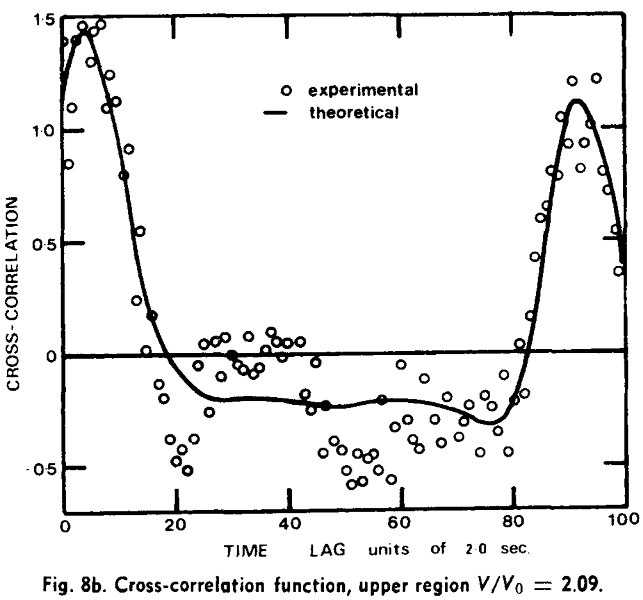

Fig. 8b. Cross-correlation function, upper region $V/V_0 = 2.09$.

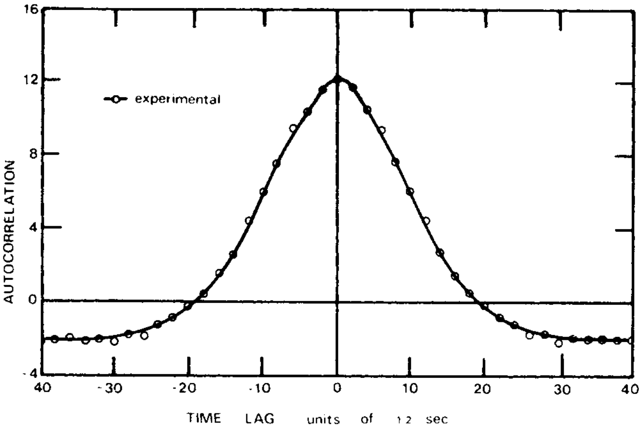

Fig. 9a. Autocorrelation function, lower region $V/V_0 = 1.55$.

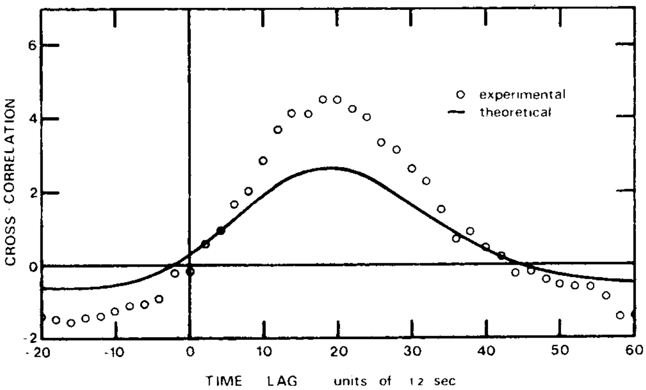

Fig. 9b. Cross-correlation function, lower region $V/V_0 = 1.55$.

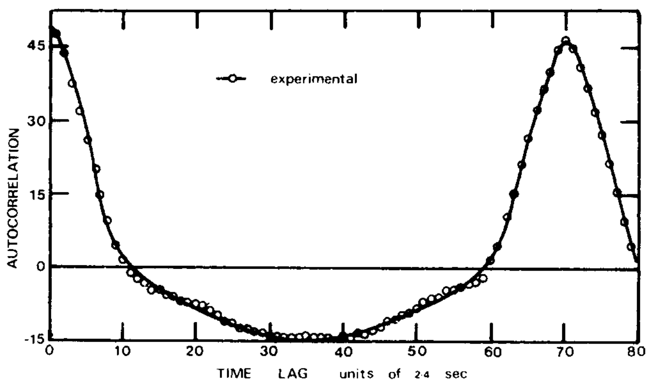

Fig. 10a. Autocorrelation function, lower region $V/V_0 = 2.09$.

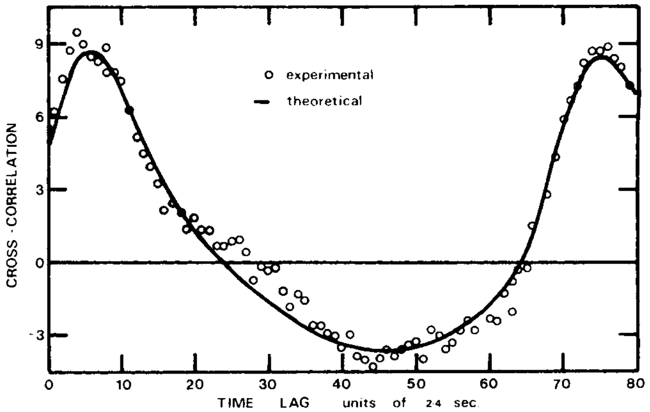

Fig. 10b. Cross-correlation function, lower region $V/V_0 = 2.09$.

in amplitude can be seen in Figure 9. The consistency in spread was checked by a nonlinear regression on the observed correlation functions by use of Equation (25). The regressed estimates of the dispersion coefficient E_1^* were found to be within 14 and 10% of the predicted values respectively.

COMPARISON WITH PREVIOUS INVESTIGATIONS

Testing of the model requires simultaneous measurement of bubble frequency and solids dispersion as a function of the operating variables. The only investigators who have carried out similar experiments are Kunii et al. (3). Values of E_1^* were calculated from the stochastic model by use of their estimates of λ and of values of D_b calculated from Equation (26), again by use of their reported values of ρ_p, D_p, and h. These are compared in Figure 11 with the observed values of the same authors and with values predicted by their bubbling-bed model. The predictions of the stochastic model compare very favorably with their work.

This comparison was made with their reported data on a microspherical catalyst, the density of which was obtained from a previous publication. They also carried out experiments on a cracking catalyst, but apparently on no occasion has the density of this material been reported. Only an indirect comparison can therefore be made, and this was done from a calculation of the particle density on the assumption that the model is valid. This value was found to be 1.34 g/cm^3, which compares favorably with values quoted by manufacturers.

SUMMARY AND CONCLUSIONS

A stochastic model was developed that predicts the local dispersion of the solids in terms of the bubble frequency and bubble diameter in a freely bubbling fluidized bed. The predictions were confirmed by experimental measurements of dispersion and they are consistent with the results of previous investigations. The stochastic model was based on the equations of motion for a single particle and should prove useful for the description of the fluidized bed reactor especially in problems associated with catalyst decay in reactor-regenerator configurations.

The model emphasizes the need to investigate the mechanism of the interaction between bubble and particle more completely. In particular the path followed by a particle during its passage around the bubble and in the wake is

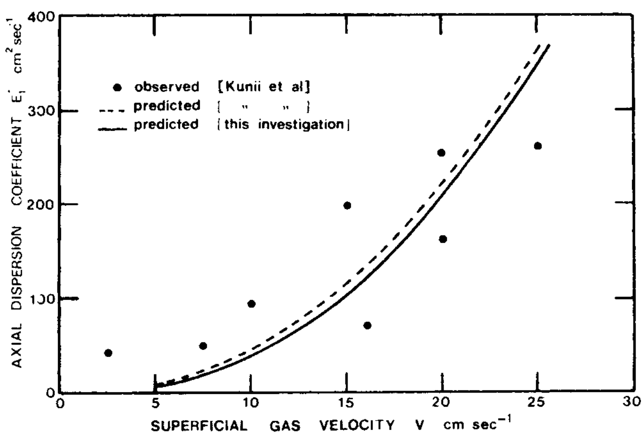

Fig. 11. Comparison with previous observations.

important for determining the vertical and lateral displacement during collision.

Although the stochastic model can be reduced in the end to an effective axial mixing model, it has two very real advantages over the deterministic model. It provides the relationship between the effective axial mixing coefficient for the solids and the measurable properties of the bubbles in the bed. This is important because the bubble motion is the dominant factor in solids dispersion. In addition the stochastic model is capable of predicting the variation of the effective mixing coefficient with bed height. It could also be modified to allow precisely for the upper and lower surfaces of shallow beds.

ACKNOWLEDGMENT

The supply of isotope by the South African Atomic Energy Board is gratefully acknowledged. This paper is published with the permission of the Director of the National Institute for Metallurgy, Johannesburg, South Africa.

NOTATION

a = axial coordinate of upper probe, cm
b = axial coordinate of lower probe, cm
D_b = bubble diameter based on equivalent sphere, cm
D_i = variance parameter for Wiener process, W_i
D_p = particle diameter, cm
$E[\cdot]$ = expectation operator
E_1 = dense phase axial diffusion coefficient, cm^2s^{-1}
E_1^* = effective axial dispersion coefficient, cm^2s^{-1}
f = Fourier transform defined by Equation (8)
$F(s)$ = distribution function for S
g = ratio of probe distances from injector a/b
h = height above distributor, cm
L = distance between probes $(b - a)$, cm
M_0, M_1, M_2 = moments of $p(x_1, t)$
$N(t)$ = Poisson process
$p(\mathbf{u}, \mathbf{x}, t)$ = joint probability density function for particle displacements and velocities
$p_x(\mathbf{x}, t)$ = probability density function for particle displacement
$p_s(s)$ = probability density function for S
$p_r(r)$ = probability density function for R
R = horizontal distance between particle and bubble flow path, cm
R_{aa} = autocorrelation function for exciting signal
S = amplitude of jump transition, cm
$\overline{S}$ = expected value of S, cm
t = time, s
$\mathbf{U}(t)$ = vector of particle velocities cm s^{-1}
U_m = downward drift, cm s^{-1}
U_s = superficial solids velocity, cm s^{-1}
$\mathbf{u}$ = coordinate of point in velocity space
v = superficial gas velocity, cm s^{-1}
v_0 = minimum superficial gas velocity for fluidization, cm s^{-1}
$\mathbf{W}(t)$ = vector of Wiener processes
$\mathbf{X}(t)$ = particle displacement, cm
$\mathbf{x}$ = coordinate position, cm
i = coordinate direction

Greek Letters

α = jump parameter, cm^{-1}
β = frictional coefficient, s^{-1}
δ = dirac delta function
λ = collision or bubble frequency, s^{-1}
θ = time, s
ρ_p = particle density, cm
τ = correlation lag, s
ξ = transformed variable

LITERATURE CITED

1. Rowe, P. N., and B. A. Partridge, "The interaction between fluids and particles," p. 135, Inst. Chem. Engrs., London (1962).
2. Gabor, J. D., *Chem. Eng. Progr. Symp. Ser., No. 62,* 35 (1966).
3. Kunii, D., K. Yoshida, and O. Levenspiel, Tripartite Chem. Eng. Conf., Montreal, Canada (1968).
4. Morris, D. R., K. E. Gubbins, and S. B. Watkins, *Trans. Inst. Chem. Engrs.*, **42,** T323 (1964).
5. Littman H., *AIChE J.*, **10,** 924 (1964).
6. Alfke, G., M. Baerns, K. Schugerl, and G. Schieman, *Chem. Ing. Tech.*, **38,** 553 (1966).
7. Sandblom, H., *Br. Chem. Eng.*, **13,** 677 (1968).
8. Uhlenbeck, G. E., and L. S. Ornstein, *Phys. Rev.*, **36,** 823 (1930).
9. Houghton, G., *Ind. Eng. Chem. Fundamentals,* **5,** 153, (1966).
10. Kunii, D., and O. Levenspiel, *Ind. Eng. Chem. Fundamentals,* **7,** 446, (1968).
11. Toei, R., R. Matsuno, and Y. Magai, Kyoto Univ. Memoirs, Faculty of Eng. **2,** 428 (1966).
12. Rowe, P. N., *Chem. Eng. Progr. Symp. Ser. No. 38,* **58,** 42 (1962).
13. Reuter, H., *ibid., No. 62,* **62,** 92 (1966).
14. Gabor, J. D., Proc. Intern. Symp. on Fluidization, A. Drinkenberg, Ed. p. 230, Neth. Univ. Press, Amsterdam (1967).
15. Lighthill, M. J., *J. Fluid Mech.*, **1,** 31 (1956).
16. Bailie, R. C., Proc. Intern. Symp. on Fluidization, A. Drinkenberg, Ed., Neth. Univ. Press, Amsterdam (1967).
17. Winter, O., *AIChE J.*, **14,** 426 (1968).
18. Park, W. H., W. K. Kang, C. E. Capes, and G. L. Osberg, *Chem. Eng. Sci.*, **24,** 851 (1969).
19. Rowe, P. N., B. A. Partridge, A. G. Cheney, G. A. Henwood, and E. Lyall, *Trans. Inst. Chem. Engrs.*, **43,** T271, (1965).
20. Cox, D. R., and H. D. Miller, "The Theory of Stochastic Processes, p. 227, Methuen, London, England (1965).
21. Feller, W., *Trans. Am. Math. Soc.*, **48,** 481 (1940).
22. Takacs, L. "Stochastic Processes," Methuen, London, England (1960).
23. Liebowitz, M. A., *J. Math. Phys.*, **4,** 852 (1963).
24. Pawula, R. F., *I.E.E.E. Trans. on Information Theory,* **33,** IT-131 (1967).
25. Papoulis, A., "Probability, Random Variables and Stochastic Processes," p. 126, McGraw Hill, New York (1965).
26. Woollard, I. N. M., and O. E. Potter, *AIChE J.*, **14,** 388 (1968).
27. Cox, D. R., and H. D. Miller, "The Theory of Stochastic Processes," p. 239, Methuen, London, England (1965).
28. Law, V. J., and R. V. Bailey, *Chem. Eng. Sci.*, **18,** 189 (1963).
29. Woodburn, E. T., *Can. J. Chem. Eng.*, **47,** 242 (1969).
30. Kato, K., and C. Y. Wen, *Chem. Eng. Sci.*, **24,** 1351 (1969).
31. Kobayashi, H., F. Arai, and T. Shiba, *Chem. Eng., Tokyo,* **29,** 858 (1965).
32. Brötz, W., *Chem. Ing. Tech.*, **24,** 60 (1952).
33. Hayakawa, T., G. Graham, and G. L. Osberg, *Can. J. Chem. Eng.*, **42,** 99 (1964).
34. Jinescu, G., I. Teoreanu, and E. Ruckenstein, *ibid.*, **44,** 73 (1966).
35. Kunii, D., K. Yoshida, and I. Hiraki, Proc. Intern. Symp. on Fluidization, A. Drinkenberg, Ed., p. 243, Neth. Univ. Press, Amsterdam (1967).
36. Kunii, D., and O. Levenspiel, "Fluidization Engineering," Wiley, New York (1969).
37. Jazwinsky, A., "Stochastic Processes and Filtering Theory," Academic Press, New York (1970).

Manuscript received June 22, 1971; revision received January 11, 1972; paper accepted January 13, 1972.